

Thermoelastic stresses in slip systems of ribbon gallium oxide crystals grown from a melt by the Stepanov method (EFG)

© V.M. Krymov, E.V. Galaktionov, S.I. Bakholdun, S.V. Shapenkov

Ioffe Institute,
194021 St. Petersburg, Russia
e-mail: V.Krymov@mail.ioffe.ru

Received April 30, 2025

Revised June 4, 2025

Accepted June 4, 2025

The influence of anisotropy of gallium oxide crystal properties on the magnitude and distribution of shear stresses in slip systems is investigated. An algorithm of calculating shear stresses for crystals of monoclinic syngony is presented. Equivalent slip systems are found. A comparison of shear thermoelastic stresses distributions in various slip systems for thin gallium oxide ribbons grown from a melt by the Stepanov method (EFG) is carried out. A correlation between shear stresses calculated in the ribbon with orientation $[010]$ ($\bar{2}10$) and the experimental data at the dislocation structure is found.

Keywords: monoclinic syngony, transition matrix, equivalent systems.

DOI: 10.61011/TP.2025.12.62373.222-25

Introduction

Crystals of β -phases of gallium oxide (β - Ga_2O_3), have been intensively studied recently and have good prospects for wide application in microelectronics and high-power electronics. Gallium oxide surpasses third-generation semiconductors in band gap and electrical breakdown value, combined with radiation resistance, excellent scintillation ability, and transparency in the UV-visible region [1]. By now, Japanese company Tamura Corp. has already started commercial production of β - Ga_2O_3 crystals grown from a melt in the form of ribbons and substrates based on them. However, it is necessary not only to develop various growing processes for obtaining high-quality defect-free crystals, but also to study structural defects and the causes of their formation. Very few such studies have been conducted for β - Ga_2O_3 crystals.

The defective structure of plates oriented parallel to the planes (010) and $(\bar{2}10)$ was studied in a number of papers [2–6] using X-ray topography, selective etching, and transmission electron microscopy. Nakai et al. [2] were the first to find two types of defects in the cross section of plates (010) : b -screw dislocations forming subgrain boundaries parallel to the planes $(\bar{2}10)$, (010) , and hollow nanotubes elongated along $[010]$. Yamaguchi et al. [3] analyzed the crystal structure of β - Ga_2O_3 based on the well-known principle that the main planes and slip directions correlate with densely packed planes and shortest translation vectors, respectively. Four slip planes have been identified: $\{\bar{2}01\}$, $\{101\}$, $\{\bar{3}10\}$, $\{\bar{3}\bar{1}0\}$ and the directions of the shortest translations in them (table, points 1.1–4.3). The existence of dislocations of the $\{\bar{2}01\}$ system has been strictly established by X-ray topography using the invisibility criterion, and for others, a dislocations rows that can correspond to them

have been demonstrated. Ueda et al. [4] discovered by the method of transmission electron microscopy a rows of edge dislocations with a Burgers vector along $\langle 010 \rangle$ corresponding to etching pits on a surface parallel to $(\bar{2}10)$; hollow nanoplates perpendicular to the plane of (010) , as well as twin plates (100) . Yao et al. [5] in a substrate with orientation (010) , using synchrotron X-ray diffraction (XRD) and X-ray topography (XRT), dislocations belonging to three more slip systems $\langle 010 \rangle \{001\}$, $\langle 201 \rangle \{10\bar{2}\}$ and $\langle 001 \rangle \{100\}$ (see table, points 5–7). Information was collected in a recent review in Ref. [6] about all known slip systems, but only the indices of one of a row of crystallographically equivalent systems are given.

However, the studies described above have not considered the causes and mechanisms of the formation of defects during the growth process. Meanwhile, studies in Ref. [7] carried out during the growth of other crystals from the melt by the Stepanov method (EFG) have shown that one of the main causes of defect formation is plastic deformation under the influence of thermal stresses in slip systems. Thermoelastic stresses were calculated for cylindrical and ribbon β - Ga_2O_3 crystals in Ref. [8,9], taking into account the anisotropy of the coefficients of elasticity and thermal expansion, but without taking into account slip systems.

In this paper, thermoelastic tangential stresses in slip systems of β - Ga_2O_3 crystals grown in the form of ribbons in the direction $[010]$ has been calculated according to the proposed algorithm, taking into account equivalent systems. Their orientation dependence in all operating slip systems has been investigated when the normal to the ribbon plane is rotated from the initial position (100) by 360° around the growing direction $[010]$.

Possible slip systems of $\beta\text{-Ga}_2\text{O}_3$ crystals

Nº	Slip Plane	Slip direction	Equivalent systems
1.1	$\{\bar{2}01\}$	$\langle 010 \rangle$	$(\bar{2}01)[010], (\bar{2}01)[0\bar{1}0], (2\bar{1})[010], (2\bar{1})[0\bar{1}0]$
1.2	$\{\bar{2}01\}$	$\langle 112 \rangle$	$(\bar{2}01)[112], (\bar{2}01)[1\bar{1}2], (2\bar{1})[\bar{1}1\bar{2}], (2\bar{1})[\bar{1}\bar{1}2]$
2.1	$\{101\}$	$\langle 010 \rangle$	$(101)[010], (101)[0\bar{1}0], (\bar{1}0\bar{1})[010], (\bar{1}0\bar{1})[0\bar{1}0]$
2.2	$\{101\}$	$\langle 10\bar{1} \rangle$	$(101)[10\bar{1}], (\bar{1}0\bar{1})[\bar{1}01]$
3.1	$\{\bar{3}\bar{1}0\}$	$\langle 001 \rangle$	$(\bar{3}\bar{1}0)[001], (\bar{3}\bar{1}0)[00\bar{1}], (\bar{3}\bar{1}0)[0\bar{0}1], (310)[00\bar{1}]$
3.2	$\{\bar{3}\bar{1}0\}$	$\langle 1\bar{3}0 \rangle$	$(\bar{3}\bar{1}0)[1\bar{3}0], (\bar{3}\bar{1}0)[130], (\bar{3}\bar{1}0)[\bar{1}\bar{3}0], (310)[\bar{1}30]$
3.3	$\{\bar{3}\bar{1}0\}$	$\langle 1\bar{3}2 \rangle$	$(\bar{3}\bar{1}0)[1\bar{3}2], (\bar{3}\bar{1}0)[132], (\bar{3}\bar{1}0)[\bar{1}\bar{3}\bar{2}], (310)[\bar{1}3\bar{2}]$
4.1	$\{\bar{3}10\}$	$\langle 001 \rangle$	$(\bar{3}10)[001], (\bar{3}10)[00\bar{1}], (\bar{3}10)[0\bar{0}1], (310)[00\bar{1}]$
4.2	$\{\bar{3}10\}$	$\langle 130 \rangle$	$(\bar{3}10)[130], (\bar{3}10)[1\bar{3}0], (310)[\bar{1}30], (\bar{3}10)[\bar{1}\bar{3}0]$
4.3	$\{\bar{3}10\}$	$\langle 132 \rangle$	$(\bar{3}10)[132], (\bar{3}10)[1\bar{3}2], (310)[\bar{1}3\bar{2}], (\bar{3}10)[\bar{1}\bar{3}\bar{2}]$
5	$\{001\}$	$\langle 0\bar{1}0 \rangle$	$(001)[0\bar{1}0], (001)[010], (001)[0\bar{1}0], (001)[010]$
6	$\{10\bar{2}\}$	$\langle 201 \rangle$	$(10\bar{2})[201], (\bar{1}02)[\bar{2}0\bar{1}]$
7	$\{100\}$	$\langle 001 \rangle$	$(100)[001], (\bar{1}00)[00\bar{1}]$

1. Algorithm for calculating tangential stresses in slip systems for ribbon crystals of monoclinic syngony

Let the slip system $\{n_1, n_2, n_3\}\langle l_1, l_2, l_3 \rangle$ be selected in the crystallographic coordinate system. Here n_1, n_2, n_3 are the crystallographic indices of the slip plane corresponding to the indices of the normal to it in the reciprocal lattice, and l_1, l_2, l_3 are the indices of the slip direction specified in the direct lattice. It should be noted that for crystals of monoclinic syngony, to which gallium oxide belongs, the crystallographic coordinate system is not Cartesian. Let's denote the vector perpendicular to the slip plane as $\mathbf{n} = (n_1, n_2, n_3)^T$, and the vector of the slip direction as $\mathbf{l} = (l_1, l_2, l_3)^T$. Further, let us denote the components of these vectors in the crystallophysical coordinates as $\mathbf{N} = (N_1, N_2, N_3)^T$ and $\mathbf{L} = (L_1, L_2, L_3)^T$, respectively, and express them in the crystallographic coordinates according to [10,11]:

$$\mathbf{N} = \frac{E\mathbf{n}}{H^*(n_1, n_2, n_3)}, \quad \mathbf{L} = \frac{(A)^T\mathbf{l}}{R(l_1, l_2, l_3)},$$

where E is the decomposition matrix of unit vectors of the crystallophysical coordinate system in basis vectors of the crystal lattice:

$$E = \begin{pmatrix} a^* & 0 & -c^* \cos \beta \\ 0 & b^* & 0 \\ 0 & 0 & c^* \sin \beta \end{pmatrix};$$

A is the decomposition matrix of the vector basis of a crystal lattice in unit vectors of a crystallophysical coordinate

system:

$$A = \begin{pmatrix} a \sin \beta & 0 & a \cos \beta \\ 0 & b & 0 \\ 0 & 0 & c \end{pmatrix};$$

H^* is the vector length \mathbf{n} in an reciprocal lattice for crystals of monoclinic syngony:

$$H^*(n_1, n_2, n_3) = (n_1^2(a^*)^2 + n_2^2(b^*)^2 + n_3^2(c^*)^2 + 2n_1n_3a^*c^* \cos(\beta^*))^{0.5};$$

R is the length of the vector \mathbf{l} in a direct lattice:

$$R(l_1, l_2, l_3) = (l_1^2a^2 + l_2^2b^2 + l_3^2c^2 + 2l_1l_3ac \cos \beta)^{0.5},$$

A, E, H^*, R are determined by the parameters of the direct and reciprocal crystal lattice. For monoclinic $\beta\text{-Ga}_2\text{O}_3$ [12] — $a = 12.214 \text{ \AA}$; $b = 3.037 \text{ \AA}$; $c = 5.798 \text{ \AA}$; $\alpha = \gamma = \pi/2$; $\beta \sim 1.812 \text{ rad}$; $a^* = 0.084 \text{ \AA}^{-1}$; $b^* = 0.329 \text{ \AA}^{-1}$; $c^* = 0.178 \text{ \AA}^{-1}$; $\alpha^* = \gamma^* = \pi/2$; $\beta^* = \pi - \beta$.

Let's find the matrix C_0 connecting the slip system and the crystallophysical coordinate system. This matrix is expressing in terms of the components of the vectors $\mathbf{N} = (N_1, N_2, N_3)^T$ and $\mathbf{L} = (L_1, L_2, L_3)^T$ as follows:

$$C_0 = C_0(n_1, n_2, n_3, l_1, l_2, l_3)$$

$$= \begin{pmatrix} N_1 & N_2 & N_3 \\ L_1 & L_2 & L_3 \\ N_2L_3 - N_3L_2 & N_3L_1 - N_1L_3 & N_1L_2 - N_2L_1 \end{pmatrix}.$$

Let us consider the ribbon $\beta\text{-Ga}_2\text{O}_3$ grown in the crystallographic direction $[010]$. The orientation of the

ribbon, in which the axis x_3 coincides with the direction of growth [010], and the axis x_1 is directed perpendicular to the plane of the ribbon and coincides with the direction (100), is considered the initial crystallophysical orientation of the plate. We construct a transition matrix from a working coordinate system to a crystallophysical system. As a working coordinate system, we choose the coordinate system obtained from the original crystallophysical system by rotating around the axis x_1 at an angle 90° counterclockwise, followed by rotating around the new axis x_3 (around the direction [010]) at an angle of ψ counterclockwise. Then the transition matrix from the working coordinate system to the initial crystallophysical system will take the form

$$C_{0R} = \begin{pmatrix} \cos \psi & 0 & \sin \psi \\ \sin \psi & 0 & -\cos \psi \\ 0 & 1 & 0 \end{pmatrix}^{-1}.$$

The transition matrix from the working coordinate system to the slip coordinate system can be written as $C = C_0 C_{0R}$. Then the tangential stresses acting in the selected slip system are determined by the following formula:

$$\tau_{12} = C_{1\alpha} C_{2\beta} \sigma_{\alpha\beta}, \quad \alpha, \beta = 2, 3,$$

where $\sigma_{\alpha\beta}$ is the tensor of thermoelastic stresses corresponding to the plane stress state. When the working coordinate system is rotated, not only the components of the matrix C_{0R} change, but also the components of the thermoelastic stress tensor $\sigma_{\alpha\beta}$, due to the anisotropy of the thermal and elastic properties of the ribbon material.

2. Calculation of tangential stresses in slip systems for ribbon crystals of gallium oxide

We find tangential stresses in a thin crystal plate $\beta\text{-Ga}_2\text{O}_3$ of length l , rectangular section $\Omega = [-b, b] \times [-h, h]$ ($2b$ — width of the ribbon, $2h$ — its thickness). Let's use the Cartesian coordinate system $(\bar{x}_1, \bar{x}_2, \bar{x}_3)$. The dimensional values are indicated by a bar at the top. The axis \bar{x}_1 is orthogonal to the ribbon plane, the axes \bar{x}_2 and \bar{x}_3 lie in the median plane, and the axis \bar{x}_3 coincides with the direction of growth. Let's proceed to dimensionless coordinates: $\bar{x}_1 = hx_1$, $\bar{x}_2 = bx_2$, $\bar{x}_3 = lx_3$. Next, we proceed to the dimensionless coefficients of thermal conductivity, thermal expansion, and elastic compliance by normalization to the corresponding invariants. To calculate the thermoelastic stresses in the ribbon, we use approximate formulas for the components $\bar{\sigma}_{33}$, $\bar{\sigma}_{23}$, and $\bar{\sigma}_{22}$ of the thermoelastic stress tensor describing the plane stress state in a thin anisotropic plate. These formulas were obtained in Ref. [13] by the method of asymptotic integration of the thermoelasticity equations under the assumption of small parameters $\delta = h/b$, $\varepsilon = b/l$ and weak heat transfer at the faces $x_1 = \pm 1$. The case of growing

a rectangular plate with a length of 0.1, width of 0.02 and thickness of 0.002m by the Stepanov method (EFG) is considered. The direction of growth is [010], the normal to the plane is [100]. To study the effect of the anisotropy of gallium oxide properties on the magnitude and distribution of tangential stresses in slip systems, the rotation of the plate around the growth axis by an angle of ψ counterclockwise was considered. Thermoelastic stresses were taken at a point with coordinates $(x_2 = 0.5, x_3)$ located in the middle part of the ribbon along its length.

3. Calculation results

All equivalent slip systems were found for the main systems listed in the following table. It was taken into account that this crystal belongs to the symmetry class $2/m$ of the monoclinic syngony and contains 2 symmetry elements: the second-order axis of symmetry and the plane of symmetry m perpendicular to it, and the effect of each symmetry element on an arbitrary crystallographic direction is described by its rotation matrix.

The results of calculations of tangential stresses for various slip systems when the plate is rotated by an angle of ψ around the growing direction [010] are shown in Fig. 1–3. Fig. 1, *a* shows a scheme of the crystal lattice of a $\beta\text{-Ga}_2\text{O}_3$ crystal with the orientation of the growing direction [010]. The ribbon plane in the scheme coincides with the slip plane $(\bar{2}\bar{1}0)$. The following scheme shows other possible slip planes: (101), $(\bar{3}\bar{1}0)$, (100), and (001). Fig. 1, *b* shows the plot of the dependence of tangential stresses in system 1.1 (the numbering of the systems is given in table) from the rotation angle ψ around the direction [010] in polar coordinates for four equivalent systems. Calculations have shown that two of the four systems match in pairs and have a different sign when the rotation angle is changed ψ . The maximum values of tangential stresses (up to 0.7 MPa) in this system are reached when the plane of the ribbon coincides with the crystallographic plane $(\bar{2}01)$, i.e. with the slip plane under consideration. Calculations in the system 1.2 also demonstrate a strong orientation dependence, but the level of tangential stresses is lower (up to 0.26 MPa).

Dependence of tangential stresses on the rotation angle ψ in systems 2.1 and 2.2 are shown in Fig. 2. These systems differ in the number of equivalent slip systems (in the first one there are four, in the second two), in addition, in the second system the stress is seven times less. It can be seen that in one slip plane, the nature of the angular dependence and the magnitudes of the tangential stresses depend on the slip direction.

Systems 3 and 4 turned out to be identical. The planes $\{\bar{3}\bar{1}0\}$ and $\{\bar{3}10\}$ differ from the others in that they are inclined relative to the direction of growth. Despite this, the polar graphs and maximum stress values for the 3.1 system (up to 0.7 MPa when rotated by 15°) turned out to be similar to the graphs and stress values in the 1.1 system (Fig. 3, *a*). The tangential stress level is significantly

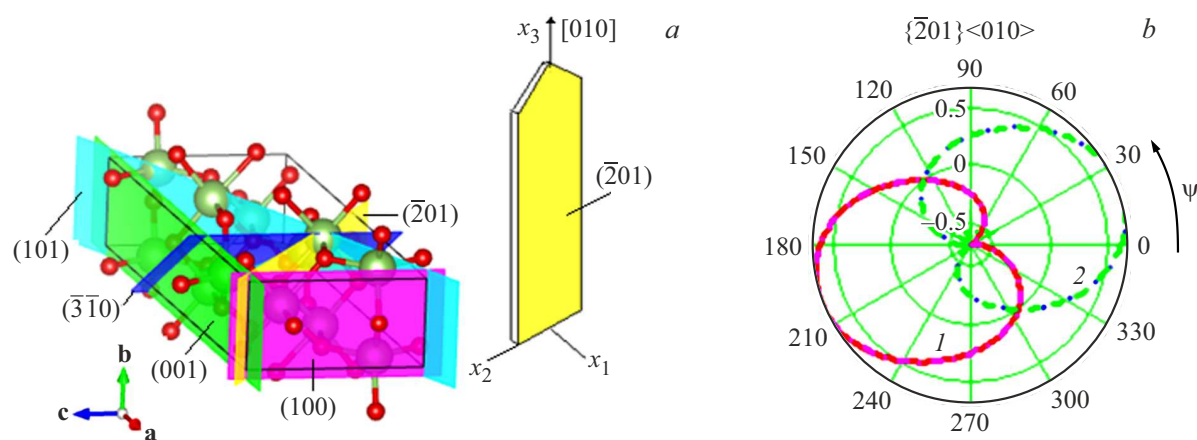


Figure 1. *a* — scheme of the ribbon and crystal cell of the crystal β — Ga_2O_3 with orientation of the growing direction $[010]$. The plane of the ribbon coincides with the slip plane $(\bar{2}01)$. The following scheme also shows other possible slip planes: (101) , $(\bar{3}10)$, (100) and (001) ; *b* — dependence of tangential stresses in the system $\{201\} <010>$ on rotation angle ψ around the direction $[010]$ in polar coordinates for four equivalent systems: 1 — slip systems $(\bar{2}01)$ [010] and (201) [010], 2 — (201) [010] and (201) [010].

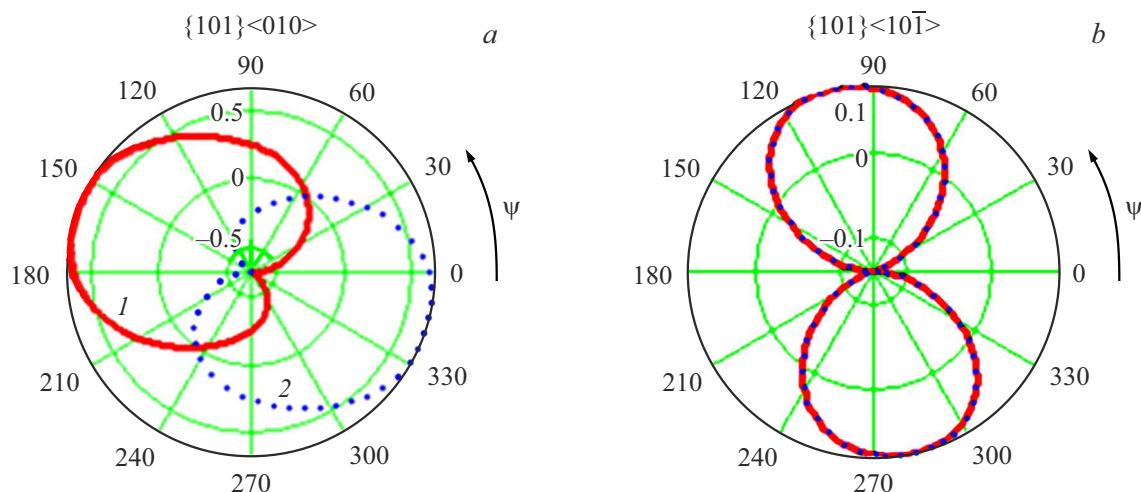


Figure 2. Dependence of tangential stresses on the angle of rotation ψ around the direction $[010]$ in polar coordinates in systems: *a* — $\{101\} <010>$ (1 — slip system (101) [010], 2 — (101) [010]); *b* — $\{101\} <10\bar{1}>$.

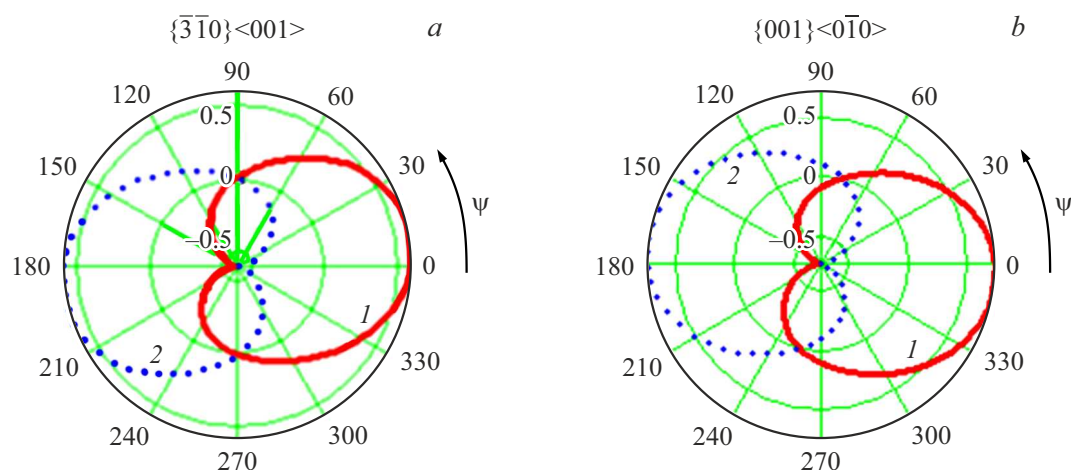


Figure 3. Dependence of tangential stresses on the angle of rotation ψ around the direction $[010]$ in polar coordinates in systems: *a* — $\{\bar{3}10\} <001>$ (1 — slip system: $(\bar{3}10)$ [001], 2 — $(\bar{3}10)$ [001]); *b* — $\{001\} <0\bar{1}0>$ (1 — (001) [010], 2 — (001) [010]).

lower (up to 0.1 MPa) in systems 3.2 and 3.3. System 5 can be distinguished among the last three systems, which gives the maximum level of tangential stresses (up to 0.74 MPa) when the ribbon plane coincides with the crystallographic plane (001) (Fig. 3, *b*). The tangential stresses are small (0.1 MPa) in systems 6 and 7.

Comparison of the calculation results with experimental data on the distribution of defects in crystals requires separate consideration. However, it can be said in advance that the calculated stresses in 1.1 and 5 systems can lead to the formation of screw dislocations found in the gallium oxide ribbons in Ref. [2].

Conclusion

An algorithm for calculating tangential stresses in slip systems for ribbon crystals of monoclinic syngony has been developed. The dependence of these stresses on the rotation of the crystallographic plane of the ribbon around the growth axis [010] for gallium oxide crystals has been studied. The calculations performed show that the magnitude and orientation of the tangential stresses in the operating slip systems depend on the initial components of the thermoelastic stress tensor and on the crystallographic structure of the crystal. In the case when there is one component in the tensor σ_{33} , it is projected only on the plane $\{\bar{3}10\}$ and $\{\bar{3}\bar{1}0\}$, and when the three components of the stress tensor are taken into account, all slip systems work. The maximum amount of tangential stresses is observed when the belt plane coincides with the slip plane.

Conflict of interest

The authors declare that they have no conflict of interest.

References

- [1] Z. Chi, J. Asher, M.R. Jennings, E. Chikoidze, A. Pérez-Tomás. *Materials*, **15** (3), 1164 (2022). DOI: 10.3390/ma15031164
- [2] K. Nakai, T. Nagai, K. Noami, T. Futagi. *Jpn. J. Appl. Phys.*, **54** (5), 051103 (2015). DOI: 10.7567/JJAP.54.051103
- [3] H. Yamaguchi, A. Kuramata, T. Masui. *Superlattices and Microstructures*, **99**, 99 (2016). DOI: 10.1016/j.spmi.2016.04.030
- [4] O. Ueda, N. Ikenaga, K. Koshi, K. Iizuka, A. Kuramata, K. Hanada, T. Moribayashi, S. Yamakoshi, M. Kasu. *Jpn. J. Appl. Phys.*, **55** (12), 1202BD (2016). DOI: 10.7567/JJAP.55.1202BD
- [5] Y. Yao, Y. Ishikawa, Y. Sugawara. *Jpn. J. Appl. Phys.*, **59** (12), 125501 (2020). DOI: 10.35848/1347-4065/abc1aa
- [6] Y. Wang, M. Zhu, Y. Liu. *China Foundry, Special Rev.*, **21**, 491 (2024). DOI: 10.1007/s41230-024-4131-5
- [7] S.I. Bakholdin, E.V. Galaktionov, V.M. Krymov. *Izv. AN, Ser. fiz.*, **63** (9), 1816 (1999) (in Russian)
- [8] S.I. Bakholdin, E.V. Galaktionov, V.M. Krymov. *Tech. Phys.*, **68** (12), 1584 (2023).
- [9] V.M. Krymov, E.V. Galaktionov, S.I. Bakholdin. *Tech. Phys.*, **69** (12), 1809 (2024).
- [10] Yu.I. Sirotin, M.P. Shaskol'skaya. *Osnovy kristallofiziki* (Nauka, M., 1979), p. 134 (in Russian).
- [11] B.K. Vajnshtejn. *Sovremennaya kristallografiya* (Nauka, M., 1979), t. 1, p. 221 (in Russian).
- [12] W. Miller, K. Böttcher, Z. Galazka, J. Schreuer. *Crystals*, **7** (1), 26 (2017). DOI: 10.3390/crust7010026
- [13] I.E. Zino, E.A. Tropp. *Asimptoticheskie metody v zadachakh teorii teploprovodnosti i termouprugosti* (Izd-vo LGU, L., 1978). (in Russian).

Translated by A.Akhtyamov